

# Metabolomic Endotypes of Age-related Macular Degeneration (AMD) Enables a Path Towards Precision Medicine



Kevin Mendez MS<sup>1,2,3</sup>, Ines Lains MD PhD<sup>1</sup>, Rachel Kelly PhD<sup>2</sup>, John Miller MD<sup>1</sup>, Demetrios Vavvas MD PhD<sup>1</sup>, Ivana Kim MD<sup>1</sup>, Joan Miller MD<sup>1</sup>, Liming Liang PhD<sup>4,5</sup>, Jessica A. Lasky-Su ScD<sup>2\*</sup>, and Deeba Husain MD<sup>1\*</sup>

<sup>1</sup>Retina Service, Massachusetts Eye and Ear, Harvard Medical School, Boston, MA, USA

<sup>2</sup>Channing Division of Network Medicine, Department of Medicine, Brigham and Women's Hospital and Harvard Medical School, Boston, MA, USA

<sup>3</sup>Centre for Integrative Metabolomics & Computational Biology, School of Science, Edith Cowan University, Perth, WA, Australia

<sup>4</sup>Program in Genetic Epidemiology and Statistical Genetics, Department of Epidemiology, Harvard T.H. Chan School of Public Health, Boston, MA, USA

<sup>5</sup>Department of Biostatistics, Harvard T.H. Chan School of Public Health, Boston, MA, USA

## PURPOSE

Age-related Macular Degeneration (AMD) has a wide spectrum of structural phenotypes. Current AMD classification is based on color photos and has phenotypic variability in each stage. We hypothesize that there are distinct AMD endotypes (i.e. subtypes defined by pathobiological mechanisms) that confer clinically meaningful differences.

Aim: To derive AMD endotypes based on metabolomics and correlate these endotypes with retinal structure and function.

## METHODS

Cohorts: Prospective, cross-sectional study including patients with AMD from 2 cohorts: Boston (n= 163) and Portugal (n= 214).

Phenotypes: All included participants were imaged with color fundus photographs and spectral domain optical coherence tomography (SD-OCT). For the US cohort dark adaptation (DA) testing was also performed.

Metabolomics: Fasting plasma samples were collected for metabolomic profiling, which was obtained using ultra-performance liquid chromatography–mass spectrometry (LC-MS) via Metabolon.

Statistical Analysis: Metabo-endotypes of AMD were identified using similarity Network Fusion (SNF) and spectral clustering. Clinical or epidemiological differences across the metabo-endotypes were explored using ANOVA and chi-squared tests. Associations with the OCT features assessed the US cohort was used as discovery cohort and then replicated in the Portuguese cohort. Metabolomics drivers of each endotype were identified based on an ANOVA and post-hoc q-values < 0.05.

## CONCLUSION

Clinically-relevant and functional endotypes of AMD can be derived using metabolomics data. By interrogating the drivers of these metabo-endotypes, there is potential to better understand the pathophysiology behind AMD as well as improve clinical classifications.

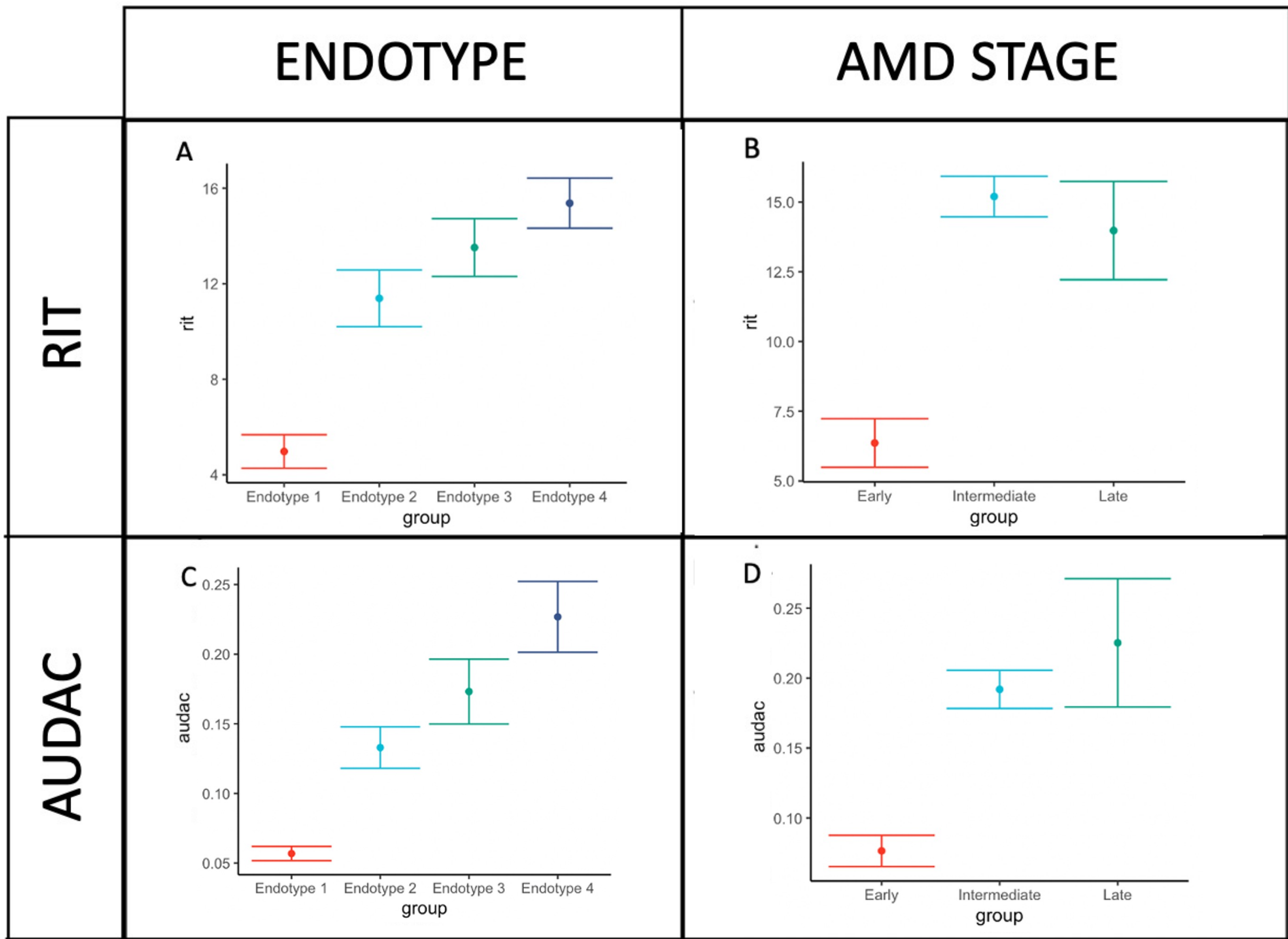
## RESULTS

We identified 4 AMD endotypes using SNF and spectral clustering with metabolomics data. AMD stage (p-value = 0.002), RIT (p-value = 0.003), and AUDAC (p-value = 0.01) significantly differed across the endotypes (Table 1). Endotype membership tracked closely to RIT but appeared to be independent of the AREDS AMD stages (Figure 1). The most important drivers of the endotypes were amino acids (isoleucine, leucine, and valine metabolites), lipid metabolites, and nucleotides (purine metabolism). Endotype 4, the most severe endotype based on dark adaptation, was broadly characterized by increased levels sphingomyelins. Endotype 3, though less severe based on RIT or AUDAC (Figure 1), has more patients with atrophy in Boston and Portugal, and EZ disruption in Portugal. While Endotype 4 was driven by high levels of levels sphingomyelins, endotype 3 was largely driven by low levels of fatty acid (acyl carnitine) metabolites.

**Table 1.** Clinical and Demographic Association with the 4 Endotypes

	P-Value (Boston) Training	P-Value (Portugal) Validation
<b>DEMOGRAPHICS</b>		
Age	0.448	0.791
Sex	0.937	0.735
BMI	0.621	0.449
Race	0.521	0.158
Smoking	0.07	0.777
AMD Stage	2.95e-06	0.02
<b>RETINAL FUNCTION</b>		
RIT	<b>0.001</b>	NA
AUDAC	<b>0.001</b>	NA
<b>RETINAL STRUCTURE</b>		
Classic Drusen	3.29e-08	0.67
Reticular Drusen Subretinal Drusenoid Deposits	0.91	0.21
Atrophy	<b>0.0009</b>	<b>0.03</b>
EZ Disruption	<b>3.65e-10</b>	<b>0.045</b>
Hyperreflective Foci	<b>1.19e-07</b>	<b>0.02</b>
Drusenoid PED	0.56	NA
Serous PED	0.65	0.72
Subretinal Fluid	0.047	0.13
Intraretinal Fluid	0.93	0.007
Fibrosis	0.45	0.01
Tubulations	0.02	0.12

**Figure 1.** Mean and standard error of rod-intercept time by (A) AMD Metabo-endotypes and (B) AMD Stage, and AUDAC by (C) AMD Metabo-endotype and (D) AMD Stage



**ENDOTYPE 1**  
(SIGNIFICANT METABOLITES)



**ENDOTYPE 2**  
(SIGNIFICANT METABOLITES)



**ENDOTYPE 3**  
(SIGNIFICANT METABOLITES)



**ENDOTYPE 4**  
(SIGNIFICANT METABOLITES)